Journal of Hydroscience and Hydraulic Engineering
Vol. 18, No.1 May, 2000, 183-193

RESPONSE OF SEDIMENT OXYGEN DEMAND AND PHOSPHATE RELEASE RATE TO A STAIRCASE CHANGE IN DO CONCENTRATION AND FLOW VELOCITY

By

T. Inoue

Department of Urban and Environmental Engineering, Kyushu University, Fukuoka, Japan

and

Y. Nakamura

Port and Harbour Research Institute, Ministry of Transport, Yokosuka, Japan

SYNOPSIS

Recent developments of instruments for field survey of water quality variations have provided precise information with relatively short time intervals. In eutrophic lakes and estuaries, rapid changes in dissolved oxygen (DO) concentration in the bottom layer have been reported. As DO concentration near the bottom is a key parameter controlling material transport through the sediment-water interface, such a rapid change of DO concentration may affect short term material cycling of, e.g., oxygen and phosphorus. In this study, a dynamic model which can simulate time variations of sediment oxygen demand (SOD) and phosphate release rate has been developed. This theoretical model consists of four diffusion equations of DO, phosphate, ferrous iron and sulfide. No biochemical reaction is assumed in the overlying water and mass fluxes are calculated from concentration gradients immediately above the sediment surface. According to this model, a staircase change in DO concentration in the overlying water and a staircase change in shear velocity lead to drastic changes in SOD and phosphate release rate within ~30 minutes after the change, which suggest that investigations on the transient state with a time scale of ~30 minutes is very important to understand mass balances between the water column and the sediment. On the contrary, concentration profiles in the sediment pore water do not reach a steady state within half a day. The difference in response time is caused by a difference between the time scale of diffusion in the water boundary layer and of bio-chemical reactions in the sediment. Phosphate transfer from water to sediment can occur under aerobic conditions in surface of sediment, as pointed out by Slomp *et al.* (9) for North Sea continental margin sediments. Our model satisfactorily simulated experimental results of the temporal variations in DO concentration.

INTRODUCTION

In shallow eutrophic lakes, water quality changes frequently due to stratification-destratification cycling, according to the following mechanism; 1. stratification due to temperature and solute concentration gradients; 2. anoxia in the overlying water due to high oxygen consumption in the sediment and/or the water column; 3. nutrient release from sediment; 4. destratification due to wind-induced mixing and nutrient supply to upper layer. For example, stratification develops in Lake Shinji, which is a shallow lagoon in Japan, as salty water from the sea often intrudes into the bottom layer of the lake during the passage of an atmospheric low pressure. Under stratified conditions, dissolved oxygen (DO) concentration in overlying water near the bottom depletes within usually three or four days, which causes an increase of nutrient release from the sediment (5). When a strong wind (e.g. ~10 m/sec.) keep blowing for more than several hours, wind-induced turbulence destroys the stratification (2), and the bottom water enriched with nutrients is mixed with the upper water. From a field

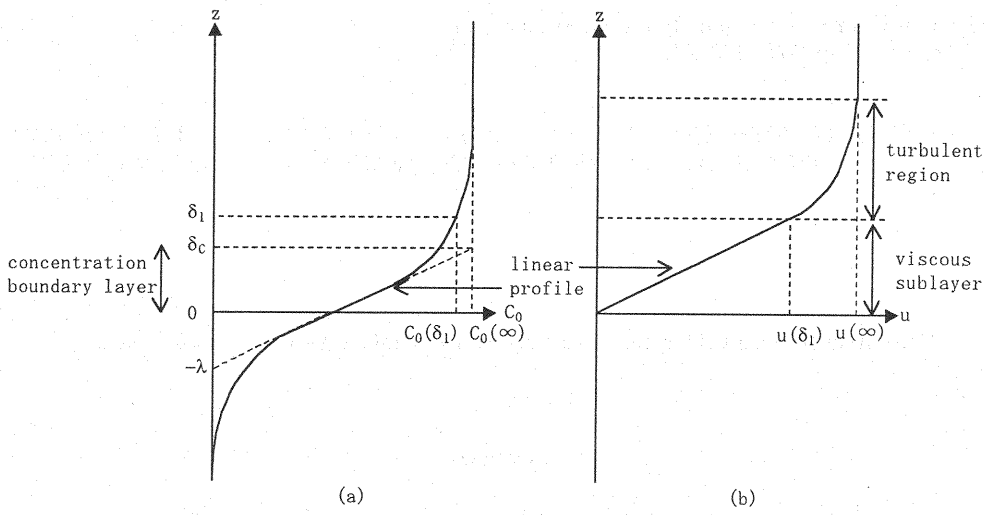

Fig.1 Schematic distributions of: (a) DO; and (b) flow velocity. In this study, the boundary layers are assumed to be fully developed. The thickness of the concentration boundary layer, δ_c, is defined by the concentration gradient at $z \rightarrow +0$ and $C(\infty)$. The length scale of the concentration profile in the sediment, λ, is defined by the concentration gradient at $z \rightarrow -0$.

observation in November 1997, Nakamura *et al.* (6) found that DO concentration measured close to the bottom sediment increased from 1 mg/l to 7 mg/l within three hours by wind-induced mixing. On one occasion, DO concentration in the bottom water rapidly decreased from nearly saturation concentration to an anoxic level after the wind stopped blowing. This phenomenon was attributed to intrusion of stratified water, which had remained in the upwind side of the lake. Furota (1) reported a rapid stratification and anoxia in Tokyo Bay, and pointed out the harmful influence of a rapid anoxia in the bottom layer on benthos. These rapid physical and chemical changes of the overlying water should affect material circulation in eutrophic shallow water areas. However, most of the previous studies on sediment oxygen demand (SOD) and nutrient release from sediment have concerned long time scales like seasonal variations, and there are few studies on the short time scale processes. The purpose of this study, therefore, is to develop a non-steady numerical model to investigate responses of SOD and phosphate release rate to rapid changes in DO concentration and flow velocity of the overlying water.

In general, solute concentration gradients exist in a boundary layer immediately above the sediment-water interface, hereinafter called a concentration boundary layer (Fig.1). Estimation of the concentration profile in the layer is essential for modeling, as the layer can act as a region of impedance to scalar transport. Recent development of oxygen microelectrodes showed that the thickness of the concentration boundary layer is typically 1 mm or less, which is thinner than the viscous sublayer (Joergensen and Des Marais (4); Nakamura and Stefan (8)). In the following analysis, the boundary layer will be treated as fully developed, because of the typically large horizontal dimensions of lakes or estuaries relative to the thickness of the concentration boundary layer.

NUMERICAL MODEL

Basic Assumptions

Our model consists of two parts: a diffusion model of the concentration boundary layer (Fig.1) and a transport/reaction model of the sediment. Nakamura and Mikogami (7) constructed a steady-state model of dissolved oxygen, phosphate and ferrous iron transfer, combining analytical solutions of their profiles in the concentration boundary layer with those in the interstitial water of sediments. For the water boundary layer, they made the following assumptions;

1. the sediment is a fixed, smooth flat bed,
2. concentrations and velocities are horizontally homogeneous,
3. the boundary layer is thin enough to ignore internal chemical/biological reactions.

The concept of the present model is based on the idea of Nakamura and Mikogami (7). However, a non-steady term was incorporated into their model to study responses of SOD and phosphate release rate to rapid variations in flow velocity and DO concentration. Terms related to sulfide reactions, which are important for sediments in saline or brackish water regions, are also included in the model.

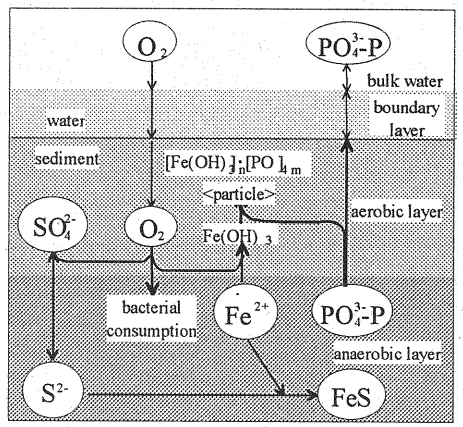

Fig.2 The concept of numerical model

Outline of the Model

DO is supplied to sediment from overlying water by diffusion in the concentration boundary layer, and consumed by chemical and bacterial reactions in the sediment. In this study, oxidation of ferrous iron and sulfide are considered as chemical DO consumption. Phosphate in pore water is supplied by desorption from sediment particles, and transported by molecular diffusion to the sediment surface layer. Only part of the phosphate can be transported by diffusion to the overlying water through the aerobic layer, because phosphate is adsorbable to ferric hydroxide. Ferrous iron is also supplied by desorption from sediment particles, but is consumed either by oxidation to ferric hydroxide or by reaction with sulfide. Sulfide is supplied by sulfate reduction in the anaerobic layer, while it is oxidized again to sulfate in the aerobic layer when transported by diffusion. All processes included in the present model are schematically given in Fig.2.

Basic Equations

We expressed the mass balance equations for DO, phosphate, ferrous iron and sulfide as follows, taking diffusion and biochemical reactions stated above into account.

$$\varepsilon\frac{\partial C_O}{\partial t}=\varepsilon D_{zO}\frac{\partial^2 C_O}{\partial z^2}-\frac{1}{4}\varepsilon k_{OF}C_O C_F-k_B C_O-2\varepsilon k_{OS}C_O C_S \tag{1}$$

$$\varepsilon\frac{\partial C_P}{\partial t}=\varepsilon D_{zP}\frac{\partial^2 C_P}{\partial z^2}-\alpha\varepsilon k_{OF}C_O C_F-k_{ad}\left[C_P-C_P(-\infty)\right] \tag{2}$$

Table.1 Parameter values applied in the model

Figs.	shear velocity (mm/sec)	kinematic viscosity(mm^2/sec)	molecular diffusion coefficient (mm^2/sec) DO	PO_4-P	Fe	S	ε
Figs.2,3	0.5	0.8	1.3×10^{-3}	4.6×10^{-4}	4.6×10^{-4}	7.0×10^{-4}	0.8
Fig.4	various	0.8	1.0×10^{-3}	3.6×10^{-4}	3.6×10^{-4}	7.0×10^{-4}	0.9
Fig.5	various	0.818	2.6×10^{-3}	3.6×10^{-4}	3.6×10^{-4}	7.0×10^{-4}	0.875
Figs.6,7,8	0.5→3.0	0.8	1.3×10^{-3}	4.6×10^{-4}	4.6×10^{-4}	7.0×10^{-4}	0.8
Figs.9,10,11	1.5	0.818	2.6×10^{-3}	4.6×10^{-4}	4.6×10^{-4}	7.0×10^{-4}	0.875

Figs.	k_{OF} (mm^3/m	k_B (1/sec)	k_{OS} (mm^3/mmol/sec)	k_{ad} (1/sec)	k_{FS} (mm^3/mmol/sec)	k_S (mmol/mm^3/sec)	α
Figs.2,3	11500	0	0	1.0×10^{-4}	0	0	1
Fig.4	100000	0	0	1.0×10^{-5}	0	0	1
Fig.5	308253	0.023	0	1.0×10^{-4}	0	0	14
Figs.6,7,8	11500	0	0	1.0×10^{-4}	0	0	1
Figs.9,10,11	308253	0.023	0	1.0×10^{-4}	0	0	14

Figs.	C_O(z=-30mm) (mg/l)	C_P(z=-30mm) (mg/l)	C_F(z=-30mm) (mg/l)	C_S(z=-30mm) (mg/l)	C_O(z=10mm) (mg/l)	C_P(z=10mm) (mg/l)	C_F(z=10mm) (mg/l)	C_S(z=10mm) (mg/l)
Figs.2,3	0	3.10	5.58	0	various	0.31	0.558	0
Fig.4	0	3.90	7.04	0	0	0	0	0
Fig.5	0	2.42	0.31	0	1.08	0.048	0.006	0
Figs.6,7,8	0	3.10	5.58	0	7	0	0	0
Figs.9,10,11	0	2.42	0.31	0	0→7	0.02	0.003	0

$$\varepsilon \frac{\partial C_F}{\partial t} = \varepsilon D_{zF} \frac{\partial^2 C_F}{\partial z^2} - \varepsilon k_{OF} C_O C_F - \frac{1}{\alpha} k_{ad} \left[C_P - C_P(-\infty) \right] - \varepsilon k_{FS} C_F C_S \quad (3)$$

$$\varepsilon \frac{\partial C_S}{\partial t} = \varepsilon D_{zS} \frac{\partial^2 C_S}{\partial z^2} + \varepsilon k_S - \varepsilon k_{FS} C_F C_S - \varepsilon k_{OS} C_O C_S \quad (4)$$

where C_O, C_P, C_F, C_S = concentrations of DO, phosphate, ferrous iron and sulfide, respectively; D_{zO}, D_{zP}, D_{zF}, D_{zS} = diffusion coefficient of DO, phosphate, ferrous iron and sulfide, respectively; t = time; z = vertical axis from the sediment-water interface (positive upward and zero at the sediment-water interface); ε = porosity; k_{OF} = rate constant of ferrous iron oxidation; k_B = oxygen consumption rate constant by bacteria; k_{OS} = rate constant of sulfide oxidation; k_{ad} = phosphate adsorption rate constant; k_{FS} = reaction rate constant of ferrous iron and sulfide; k_S = production rate constant of sulfide; α = number of moles of phosphate adsorbed per unit mole of ferric hydroxide; and $C_P(-\infty)$ = phosphate concentration in pore water at z = - ∞.

The left-hand side of each equation indicates the rate of change in concentration, and the first term on the right-hand side indicates diffusive transport. In Eq. 1, the second term on the right-hand side represents the DO consumption due to oxidation of ferrous iron, the third term is the bacterial consumption, and the fourth term represents the DO consumption due to oxidation of sulfide. For Eqs. 2 and 3, the second and third terms on the right-hand side denote the adsorption to and desorption from sediment particles, respectively. The fourth term in Eq. 3 represents the reaction of ferrous iron and sulfide. The second term in Eq. 4 represents the production of sulfide due to reduction of sulfate, the third term is the decrease of sulfide by reaction with ferrous iron, and the fourth term represents the decrease by oxidation. Note that the basic equations from (1) to (4) are applied for both water boundary layer and the sediment, whereas, reaction terms are ignored in the water boundary layer because of its small scale.

The diffusion coefficients are assumed as follows,

$$D_z = D_{zm} + D_{zt} \quad (\text{for } z \geq 0) \quad (5)$$

$$D_z = D_{zm} \quad (\text{for } z < 0) \quad (6)$$

$$\frac{D_{zt}}{\nu} = \left(A_m \frac{z u_*}{\nu} \right)^m \quad (7)$$

where D_z = vertical diffusion coefficient; D_{zm} = molecular diffusion coefficient; D_{zt} = turbulent diffusion coefficient; ν = kinematic viscosity; u_* = shear velocity; and A_m(= 0.078), m(= 3) = numerical constants (Nakamura and Mikogami (7)).

Boundary Conditions and Parameter Values

As our primary concern is variations of solute concentrations near the sediment-water interface within relatively short time scales, concentrations far away from the interface can be considered to be constant. In the calculations, fixed concentrations of solutes at z = 10 mm for the water layer and z = - 30 mm for the sediment layer are used as boundary conditions, except for the moment of the staircase change in concentrations. Values of parameters are given, following Ishikawa and Nishimura (3) and Nakamura and Mikogami (7). Diffusion coefficients for sediment pore water are different from the molecular diffusion coefficient in the water because of tortuosity. Concerning sediment with high porosity, however, the difference can be ignored, as the order is considered as the square of the porosity.

RESULTS AND DISCUSSION

Concentrations of dissolved materials in pore water are affected by the flow velocity of the overlying water and the redox potential in the sediment. Four kinds of calculation results are given in the following sections. The first section includes results of steady-state calculations under various DO concentrations as upper boundary condition. The second section also presents results of steady-state calculations, under the condition of various flow velocities. The results of non-steady calculations for a staircase change in flow velocity are given in the third section, and those for a staircase change in DO concentration are given in the fourth section. In these

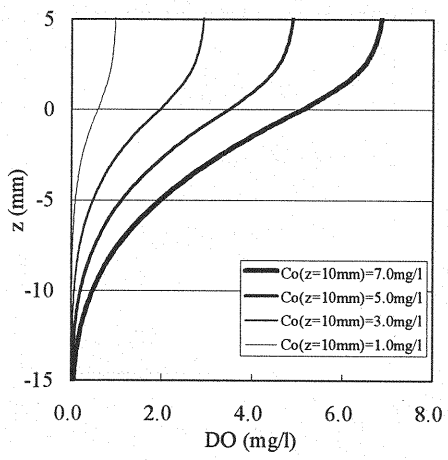

Fig.3 DO concentration profiles as a function of $C_O(z=10mm)$

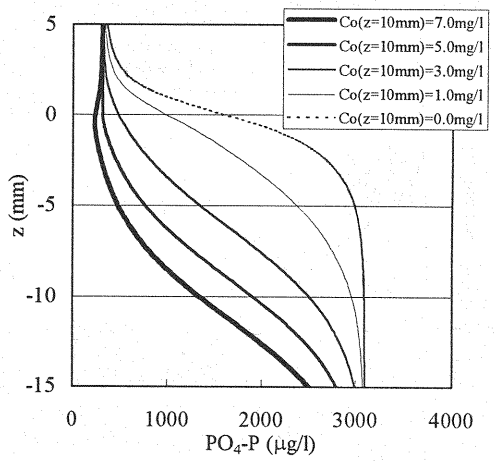

Fig.4 Phosphate concentration profiles as a function of $C_O(z=10mm)$

calculations, the upper boundary conditions are given at z = 10 mm and the lower at z = - 30 mm. For the case of a staircase change in flow velocity, the shear velocity, rather than the flow velocity itself, is changed in the calculations. The effect of transient variations in flow structure (variation in turbulence intensity and the thickness of the viscous sublayer) are ignored, as the time scale of momentum transfer in the boundary layer is generally much shorter than that of transfer/reactions of solutes.

Effect of DO Concentration (Steady State)

In this section, we discuss the effect of DO concentration in the overlying water ($C_O(z = 10\ mm)$) on DO ($C_O(z)$) and phosphate ($C_P(z)$) concentration profiles in a steady state (Figs.3, 4 and 5). Fig.3 shows the calculated results of DO concentration, $C_O(z)$, around the interface (z = 0) as a function of $C_O(z = 10\ mm)$ (from 0 mg/l to 7 mg/l) as the upper boundary condition. In this calculation, 10% of the values of $C_P(z = -30\ mm)$ and $C_F(z = -30\ mm)$ (= 100 μmol/l) were given as $C_P(z = 10\ mm)$ and $C_F(z = 10\ mm)$ (= 10 μmol/l), respectively (Table.1). The thickness of the concentration boundary layer was constantly about 3 mm. However, $\partial C_O/\partial z$ at z = 0 increases as $C_O(\infty)$ increases. Since diffusive fluxes of dissolved materials are defined as $D_z(\partial C/\partial z)$, an increase of $C_O(z = 10\ mm)$ implies an increase of SOD. As a result, the depth of DO penetration also increases as $C_O(z = 10\ mm)$ increases.

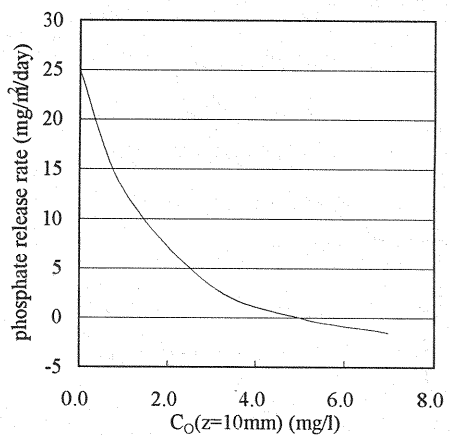

Fig.5 Phosphate release rate as a function of $C_O(z=10mm)$

Fig.4 shows profiles of phosphate concentrations, $C_P(z)$, as a function of $C_o(\infty)$. Under anaerobic conditions ($C_o(z)$ = 0 mg/l), the phosphate concentration gradient, $\partial C_P/\partial z$, at z = 0 was steepest, which means a maximum phosphate release rate. As $C_O(\infty)$ increased, the magnitude of the phosphate gradient at the interface decreased and thus the phosphate release rate decreased (see also Fig.5). At high $C_O(\infty)$, the gradient became positive (the case $C_o(z = 10\ mm)$ = 7 mg/l in Fig.4). This means that sorption of phosphate from the water to the sediment can occur under aerobic conditions. This is due to the decrease of $C_P(z)$ in the aerobic surface layer of the sediment (Fig.2), caused by a rapid oxidation of the sediment surface. This result suggests that sediment may be a sink of phosphate depending on DO concentration. In all cases showed in Figs.3 and 4, the thickness

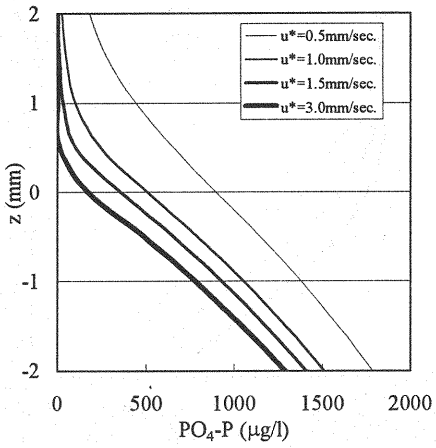

Fig.6 Phosphate concentration profiles as a function of shear velocities (Anaerobic condition)

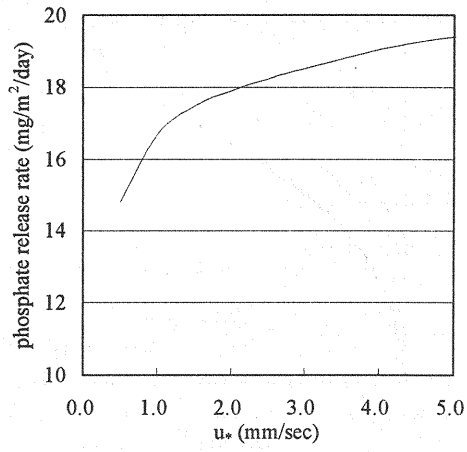

Fig.7 Phosphate release rate as a function of shear velocities (Anaerobic condition)

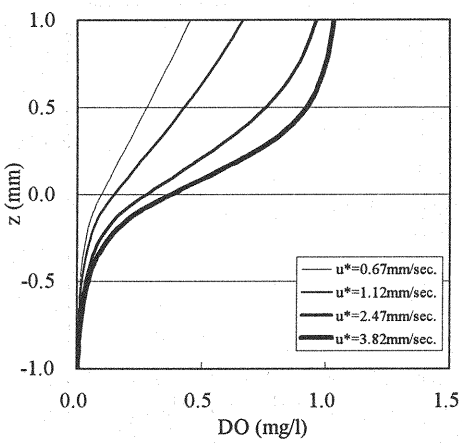

Fig.8 DO concentration profiles as a function of shear velocities (Low DO concentration condition)

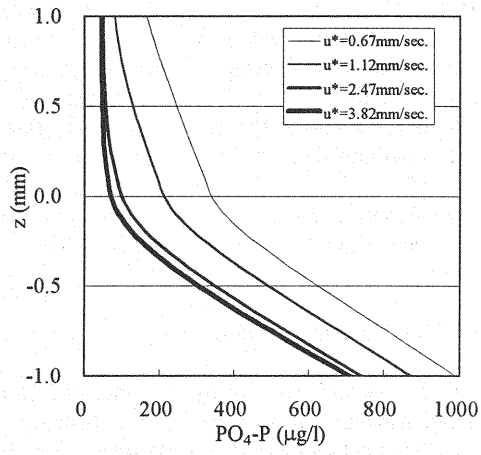

Fig.9 Phosphate concentration profiles as a function of shear velocities (Low DO concentration condition)

of the concentration boundary layer was constant, as shear velocity was kept constant.

Effect of Flow Velocity (Steady State)

In this section, effects of flow velocity of the overlying water on DO and phosphate concentration profiles ($C_O(z)$ and $C_P(z)$) in a steady state are studied (Figs.6-10). Fig.6 shows calculated results of $C_P(z)$ around the interface for various u_* (from 0.5 to 3.0 mm/sec) under anaerobic conditions ($C_O(z)$ = 0 mg/l). As u_* increased, the concentration boundary layer thickness decreased , while $\partial C_P / \partial z$ in the boundary layer increased. These results show that phosphate release rate increases as u_* increases under anaerobic conditions (Fig.7), and support the analytical results obtained by Nakamura and Mikogami (7). Figs.8 and 9 show the calculated results of $C_O(z)$ and $C_P(z)$, respectively, for various u_* (from 0.5 to 3.0 mm/sec) under low DO concentration conditions ($C_O(\infty)$ = 1 mg/l). The concentration boundary layer thickness decreased with increasing u_*, as was the case for anaerobic conditions. However, the relationship between phosphate flux and u_* was opposite. As the increase of SOD

made the sediment surface aerobic (Fig.8), due to the increase of flow velocity, adsorption of phosphate became active and thus the concentration $C_P(z)$ in the pore water of the sediment surface layer decreased (Fig.9). As a result, phosphate release rate decreased as flow velocity increased (Fig.10).

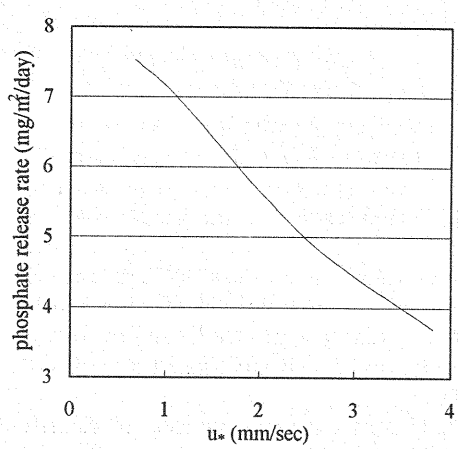

Fig.10 Phosphate release rate as a function of shear velocities (Low DO concentration condition)

Response to a Staircase Change in Flow Velocity

We examined the response of DO and phosphate concentration profiles ($C_O(z)$ and $C_P(z)$) and fluxes to a staircase increase in flow velocity. Figs.11 and 12 show the response of $C_O(z)$ and $C_P(z)$, respectively, to a staircase change of u_* from 0.5 to 3.0 mm/sec. These are the results of non-steady calculations with $u_* = 3.0$ mm/sec, by using steady-state profiles with $u_* = 0.5$ mm/sec as initial conditions. The variation of $C_P(z)$ is almost the mirror image of $C_O(z)$. $C_O(z)$ and $C_P(z)$ in the water layer ($z>0$) reached steady state in 15 minutes, whereas corresponding profiles in the sediment pore water ($z<0$) did not arrive at a steady state until after half a day. This is due to that the time scale of transport affected by biochemical reactions in the sediment is larger than that of diffusion in the water.

Let us define the time scales of diffusion in the concentration boundary layer, τ_d (Eq.8), diffusion in the sediment, τ_s (Eq.9), desorption of phosphate, τ_{ad} (Eq.10), and DO consumption due to oxidation of ferrous iron, τ_o (Eq.11), respectively, as,

$$\tau_d = \delta_c^2 / D_{zm} \tag{8}$$

$$\tau_s = \lambda^2 / D_m \tag{9}$$

$$\tau_{ad} = 1/k_{ad} \tag{10}$$

$$\tau_o = 1/k_{OF} C_F(-\infty) \tag{11}$$

where δ_c = thickness of concentration boundary layer; λ = length scale of concentration profile in the sediment; D_{zm} = molecular diffusion coefficient; $C_F(-\infty)$ = ferrous iron concentration in pore water at $z = -\infty$. The values of δ_c and λ are theoretically given by simplified analysis as follows (Nakamura and Mikogami (7); Ishikawa and

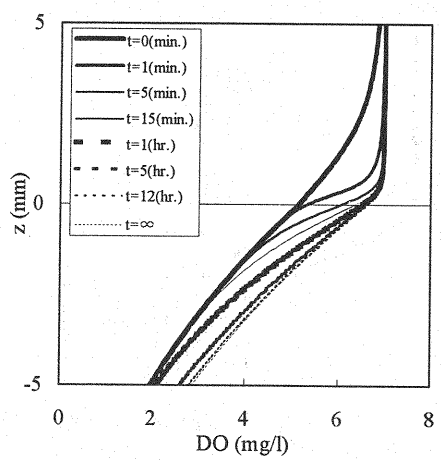

Fig.11 DO concentration profiles after the staircase increase in shear velocity

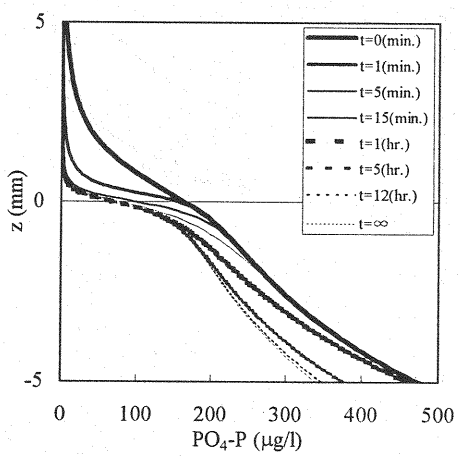

Fig.12 Phosphate concentration profiles after the staircase increase in shear velocitv

Nishimura (3)).

$$\delta_c = 15.5\, Sc^{2/3} (D_{zm} / u_*) \qquad (12)$$

$$\lambda = (\varepsilon D_{zm} / k_{ad})^{1/2} \qquad (13)$$

where Sc ($=\nu/D_{zm}$) is the Schmidt number.

For the case of $u_* = 3.0$ mm/sec, τ_d (= 2.4 minutes for DO) is smaller than τ_s (= 681 minutes). This difference makes the response of the profile in the water faster than that in the sediment. For the whole concentration profile, it takes about half a day to reach a steady state, because the time scale of diffusion in the sediment is 681 minutes, which is longer than those of other reactions (τ_{ad} = 167 minutes and τ_o = 14.6 minutes).

Fig.13 shows the time variation of diffusive fluxes of DO and phosphate at z = 0 mm and z = 10 mm under the same calculation conditions as Figs.11 and 12. Note that DO flux is defined to be positive downward, whereas phosphate flux is positive upward. From Fig.13, firstly, we can see that diffusive fluxes at z = 0 mm have their maximum values several minutes after a staircase increase of shear velocity. The values are about 2.7 times larger for DO and 1.7 times larger for phosphate, than those in the steady state ($t \rightarrow \infty$). On the other hand, the diffusive fluxes at z = 10 mm, immediately above the concentration boundary layer, have much larger values a few minutes after the staircase change. The extreme increase of diffusive flux of phosphate is due to the rapid upward transport of accumulated phosphate within the concentration boundary layer by turbulent diffusion. Further the extreme increase of diffusive flux of DO leads to rapid accumulation of DO in the concentration boundary layer. The time integrated diffusive fluxes for 5 minutes immediately after a staircase change are 3.9 mg/m^2 for DO and 0.24 mg/m^2 for phosphate, which are almost equivalent to the diffusive transport during 1 hour in the steady state. These results clearly show that estimation based on a steady-state analysis underestimates the SOD and phosphate release rates, and thus underline the importance of considering the transient state.

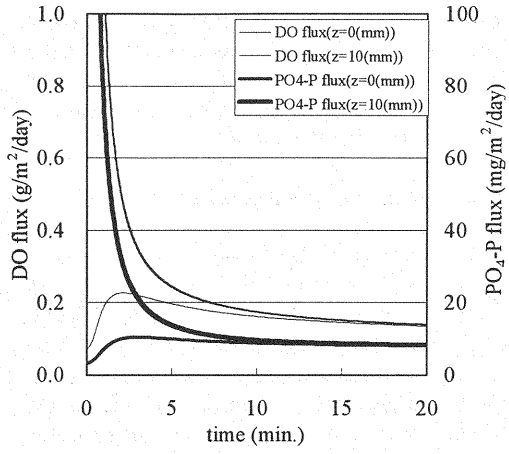

Fig.13 Time courses of diffusive fluxes after the staircase increase in shear velocity

Response to a Staircase Change in DO Concentration in Overlying Water

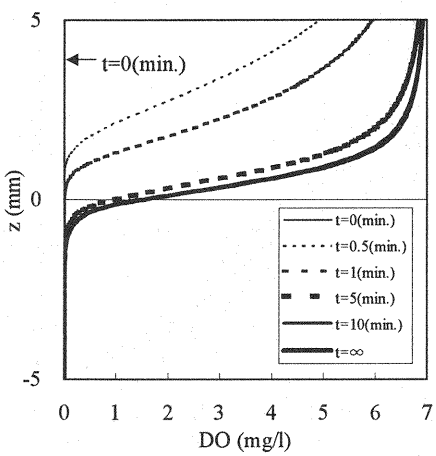

Fig.14 DO concentration profiles after the staircase increase in C_O(z=10mm)

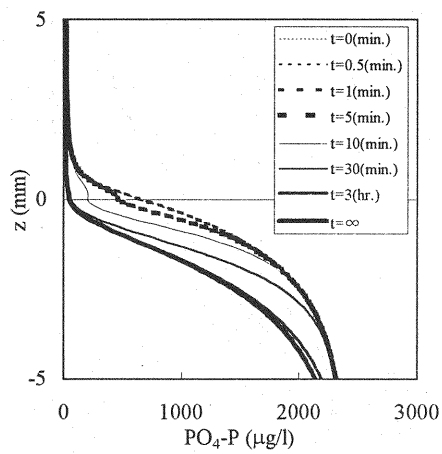

Fig.15 Phosphate concentration profiles after the staircase increase in C_O(z=10mm)

Finally, we studied the response of $C_O(z)$, $C_P(z)$ and material fluxes to a staircase increase of $C_O(z = 10\ mm)$. This condition corresponds to destratification, for example, due to wind-induced mixing which leads to a rapid increase of $C_O(z)$ at $z > 0$. Figs.14 and 15 show the $C_O(z)$ and $C_P(z)$, respectively, corresponding to a staircase change of $C_O(z = 10\ mm)$, from 0 mg/l to 7 mg/l. Initial profiles were given as solutions for C_O = 0 mg/l. $C_O(z)$ around z = 0 increased monotonously, and reached a steady state about 10 minutes after the change (Fig.14). On the other hand, it took about 3 hours for $C_P(z)$ to reach a steady state (Fig.15). The profile of $C_P(z)$ started to vary after that of $C_O(z)$ had almost reached at steady state. The delayed response of $C_P(z)$ is due to that the response of $C_O(z)$ is predominantly governed by the diffusion in the concentration boundary layer (τ_d = 9.1 minutes), while the response of $C_P(z)$ is governed by the chemical reaction (adsorption) after DO has penetrated into the sediment (τ_{ad} = 167 minutes). Furthermore, $C_P(z)$ at t = 10 min. had a positive gradient around z = 0, which means that there was a negative diffusive transport of phosphate, i.e. sorption, from the overlying water to the sediment. This phenomenon was caused by a loss of $C_P(z)$ due to adsorption to ferric hydroxides exceeding the diffusive transport, when a rapid oxidation of the sediment took place.

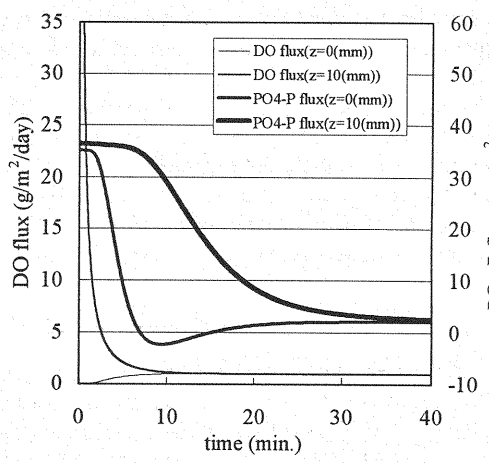

Fig.16 Time courses of diffusive fluxes after the staircase increase in $C_O(z=10mm)$

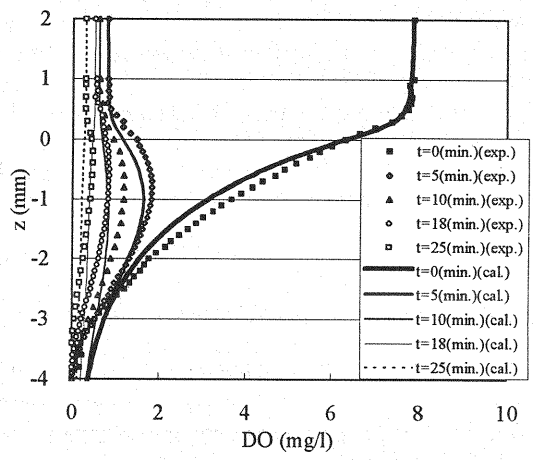

Fig.17 DO concentration profiles after the decrease in DO concentration

Fig.16 shows the response of diffusive fluxes of DO and PO_4-P at z = 0 mm and z = 10 mm under the same calculation conditions as Figs.14 and 15. We can see that the diffusive fluxes of DO approach steady-state values monotonously (Fig.16). The extremely large value at z = 10 mm is due to a rapid transport to the concentration boundary layer by turbulent diffusion. On the other hand, diffusive fluxes of phosphate do not necessarily show such monotonous time variations; the flux at z = 10 mm decreases monotonously, but the flux at z = 0 mm rapidly decreases immediately after the change, reaching even negative values for about 5 minutes, and then increases gradually to a steady-state value. The different response of DO flux and PO_4-P flux, respectively, comes from the difference between the time scales of DO diffusion (τ_d = 9.1 minutes) and oxidation of ferrous iron (τ_d = 9.7 minutes), and that of phosphate diffusion (τ_d = 15.2 minutes).

Comparison with Laboratory Experiments

Yokota *et al.* (10) measured the response of the DO concentration profile around the sediment-water interface to a staircase decrease in DO concentration in overlying water, using an oxygen microelectrode. A sediment core sampled from Lake Biwa was attached to the floor of a rectangular flume (19 cm length, 12 cm width, 5 cm height), in which lake water was recirculated. Lake water sampled from the bottom layer of the lake had previously been filtered and saturated with oxygen. After the first measurement of the DO profile (t = 0 min.), the overlying water was replaced with deoxygenated water by bubbling with N_2 gas.

Fig.17 shows the experimental results and results calculated using our numerical model. Parameters

necessary for the calculation were obtained by chemical analysis and by additional experiments with sediment sampled from the same sampling point. For example, k_B and k_{ad} were determined by monitoring of DO and phosphate concentration in a mixture of lake water and suspended sediment. The comparison of calculated results with measurements shows a good agreement, especially in the water part. The predicted DO concentration in the sediment surface layer decreased slightly faster than measurements. This discrepancy is , to some extent, related to the fact that the time necessary for the measurement of the profile, typically 2 min. or more, is not short enough compared with the transient time scale of the system. Heterogeneity of the sediment may partly be the reason, and the methodology to determine parameters leave some room for improvement. However, this model can represent the response of the DO concentration profile with reasonable accuracy.

CONCLUSIONS

A dynamic model which predicts non-steady variations in SOD and phosphate release rate was developed. The model is based on mass conservation equations for dissolved oxygen, phosphate and ferrous iron. According to the model analysis, a staircase change in DO concentration at z = 10 mm and of the shear velocity in the overlying water leads to drastic changes in SOD and phosphate release rate within ~30 minutes. The reason why diffusive fluxes in the overlying water reach steady state in ~30 minutes is that diffusive fluxes are mainly governed by the response in the concentration boundary layer. On the other hand, concentration profiles in the sediment reach steady state after a time scale of about one day. The much slower change of concentration profiles in the sediment is due to the long time scales of diffusive transport and/or biochemical reactions there. These differences in time scales cause a rapid increase or decrease of diffusive fluxes at z = 10 mm immediately after the change of DO concentration in overlying water and of shear velocity. Moreover, a negative diffusive flux of phosphate from the water to the sediment is expected under highly aerobic conditions.

Calculated results of the DO concentration profile quantitatively agreed with measurements. Therefore, we conclude that our model can simulate the response of the DO concentration profile to a staircase change in DO concentration. However, methods to determine parameters leave some room for improvement.

ACKNOWLEDGEMENTS

This study was partly supported by JSPS Research Fellowships for Young Scientists.

REFERENCES

1. Furota, T. : Survival and population maintenance of macrobenthic animals in inner Tokyo Bay, Bulletin on Coastal Oceanography, Vol.28, No.2, 1991.
2. Inoue, T., Y. Nakamura, H. Murai, Y. Ishitobi, K. Kato and M. Yamamuro : Continuous observation of the wind mixing events in Lake Shinji, Proceeding of Annual Conference of the Japanese Society of Limnology, p.192, 1996.
3. Ishikawa, M. and H. Nishimura : Mathematical model of phosphate release rate from sediments concerning the effect of dissolved oxygen in overlying water, Water Research, Vol.23, pp.351-359, 1989.
4. Joergensen, B.B. and D.J. Des Marais : The diffusive boundary layer of sediments: Oxygen microgradients over a microbial mat, Limnology and Oceanography, Vol.35, pp.1343-1355, 1990.
5. Kamiya, H., Y. Ishitobi, T. Inoue, Y. Nakamura and M. Yamamuro : Origin of nutrients accumulated in the bottom water of Lake Sinji in summer, The Japanese Journal of Limnology, Vol.57, No.4, pp.313-326, 1996.
6. Nakamura, Y., T. Inoue, Y. Adachi, Y. Ishitobi, K. Kato and M. Yamamuro ; Rapid and frequent change in water quality of the overlying water of a brackish lake: Importance of unsteady release of phosphate, Proceeding of Coastal Engineering, JSCE, Vol.46, 1999.
7. Nakamura, Y. and M. Mikogami : Effect of flow velocity on phosphate release from sediment, Proceeding of Coastal Engineering, JSCE, Vol.41, pp.1081-1085, 1994.
8. Nakamura, Y. and H.G. Stefan : Effect of flow velocity on sediment oxygen demand : Theory, Journal of Environmental Engineering, ASCE, Vol.120, No.5, pp.996-1016, 1994.
9. Slomp, C.P., J.F.P. Malschaert and W.Van Raaphorst : The role of adsorption in sediment-water exchange of phosphate in North Sea continental margin sediment, Limnology and Oceanography, Vol.43, No.5, pp.832-

846, 1998.
10. Yokota, K., H. Maeda, S. Matsumoto, Y. Nakamura, T. Inoue and M. Sayama : DO concentration microprofile around the sediment-water interface, Proceeding of Annual Conference of Kinki Branch of the Japanese Society of Limnology, 1996.

APPENDIX-NOTATION

The following symbols are used in this paper:

A_m	= numerical constant (= 0.078);
C_O, C_P, C_F, C_S	= concentrations of the DO, phosphate, ferrous iron and sulfide, respectively;
$C_F(-\infty)$	= ferrous iron concentration in pore water at $z = -\infty$;
$C_P(-\infty)$	= phosphate concentration in pore water at $z = -\infty$;
D_z	= vertical diffusion coefficient;
D_{zm}	= molecular diffusion coefficient;
D_{zO}, D_{zP}, D_{zF}, D_{zS}	= diffusion coefficient of the DO, phosphate, ferrous iron and sulfide, respectively;
D_{zt}	= turbulent diffusion coefficient;
k_{ad}	= phosphate adsorption rate constant;
k_B	= oxygen consumption rate constant by bacteria;
k_{FS}	= chemical combination rate constant of ferrous iron and sulfide;
k_{OF}	= rate constant of ferrous iron oxidation;
k_{OS}	= rate constant of sulfide oxidation;
k_S	= production rate constant of sulfide;
m	= numerical constant (= 3);
t	= time;
u_*	= shear velocity;
z	= vertical axis from the sediment-water interface (positive upward);
α	= number of moles of phosphate adsorbed to the unit mole of ferric hydroxide;
δ_c	= thickness of concentration boundary layer;
ε	= porosity ;
λ	= length scale of concentration profile in the sediment;
ν	= kinematic viscosity;
τ_{ad}	= time scale of desorption of phosphate;
τ_d	= time scale of diffusion in concentration boundary layer;
τ_o	= time scale of DO consumption due to oxidation of ferrous iron; and
τ_s	= time scale of diffusion in the sediment.

(Received November 17, 1999 ; revised March 7, 2000)